ChemPubSoc Europe

DOI: 10.1002/chem.201304699

CHEMISTRY
A European Journal
Communication

Supramolecular Catalysis

Dinuclear Ru–Aqua Complexes for Selective Epoxidation Catalysis Based on Supramolecular Substrate Orientation Effects

Carlo Di Giovanni,[a] Albert Poater,*[b] Jordi Benet-Buchholz,[a] Luigi Cavallo,[c] Miquel Solà,[b] and Antoni Llobet*[a]

Abstract: Ru–aqua complex $\{[Ru^{II}(trpy)(H_2O)]_2(\mu\text{-pyr-dc})\}^+$ is a powerful epoxidation catalyst for a wide range of linear and cyclic alkenes. High turnover numbers (TNs), up to 17000, and turnover frequencies (TOF), up to 24120 h^{-1} (6.7 s^{-1}), have been obtained using PhIO as oxidant. This species presents an outstanding stereospecificity for both *cis* and *trans* olefins towards the formation of their corresponding *cis* and *trans* epoxides. In addition, it shows different reactivity to *cis* and *trans* olefins due to a substrate orientation supramolecular effect transmitted by its ligand scaffold. This effect together with the impressive reaction rates are rationalized using electrochemical techniques and DFT calculations.

Supramolecular catalysis is a very elegant and attractive strategy for the selective transformation of organic substrates that is based on non-covalent interactions between the catalyst and the substrates. In general, the design of a supramolecular transition-metal catalyst involves a multifunctional molecule or supramolecule in which one site is responsible for the substrate transformation and another side allows for the non-covalent interaction of the substrates with the catalyst. The concept has been successfully applied to a variety of catalytic reactions involving hydrogenation, hydroformylation, Henry reactions, and so on.[1–5] For oxidation reactions, successful examples are basically limited to very few reactions that involve the combination of a non-covalent binding site with a catalytically oxidative metal.[6–10] Additional examples but with limited success include complexes with exotic ligands and high molecular weights.[11,12] In the particular case of redox catalysis there is an intrinsic difficulty in controlling a catalytic cycle involving a variety of oxidation states, as it is inevitably the case for these reactions. In the examples reported in the literature, the catalysts are designed with specific side arms in which the substrate interacts through H-bonding, and thus only those substrates possessing moieties susceptible for such H-bonding interaction can be selectively oxidized. For this reason there is a need to design supramolecular redox catalysts that can operate over a more universal set of substrates ideally without the need of additional functionalities.

Herein we present the first epoxidation catalyst that very efficiently and stereoselectively transforms *cis*-olefins into their corresponding *cis*-epoxide derivatives, and in addition is capable of discriminating between *cis*- and *trans*-olefins without the need of specific exotic substrate functionalization, based on a supramolecular substrate orientation effect. Similar orientation effects reported for other reactions have been previously reported by the Reek group and others.[13]

The supramolecular catalyst developed here is a dinuclear Ru complex $\{[Ru^{II}(trpy)(H_2O)]_2(\mu\text{-pyr-dc})\}^+$, $\mathbf{2}^+$, (pyr-dc^{3-} is the pyrazolate-3,5-dicarboxylate trianion; trpy is 2,2′:6′,2″-terpyridine; see Figure 1 right for drawings) that is obtained from the hydrolysis of its acetate bridged precursor $\{[Ru^{II}(trpy)]_2(\mu\text{-pyr-dc})(\mu\text{-OOCMe})\}$, **1**, in aqueous media. These complexes have been thoroughly characterized by analytic, spectroscopic, and electrochemical techniques. An Ortep view of the crystal structure of **1** is presented in Figure 1, left. As can be observed in Figure 1, the geometry of the bridging dinucleating pyr-dc^{3-} ligand allows placing of the two metals in relatively close proximity (4.33 Å). In addition, the pyr-dc^{3-} ligand fosters the electronic communication between the two ruthenium metals through the pyrazolato moiety.[14,15] This electronic coupling is in turn responsible for the cooperative effects presented by complex $\mathbf{2}^+$. Furthermore, the combination of the meridional geometry of the trpy ligands that are situated perpendicular to the pyr-dc^{3-} ligand generates an exceptional sixth coordination for the Ru metals in such a way that potential monodentate ligands will end up with a significant through space interaction.[15–17] This through-space interaction can be inferred from the non-coplanar arrangement of the acetato bridge with regard to that of the pyrazolato moiety (36.92°). The trianionic nature of the pyr-dc^{3-} ligand acts as a very powerful electron donor to the Ru centers and thus stabilizes their high oxidation states generating the corresponding Ru=O moieties.

[a] Dr. C. Di Giovanni, Dr. J. Benet-Buchholz, Prof. A. Llobet
Institute of Chemical Research of Catalonia (ICIQ)
Av. Països Catalans 16, 43007 Tarragona (Spain)
Departament de Química
Universitat Autònoma de Barcelona Cerdanyola del Vallès
08193, Barcelona (Spain)
E-mail: allobet@iciq.cat

[b] Dr. A. Poater, Prof. M. Solà
Institut de Química Computacional i Catàlisi (IQCC)
and Departament de Química, Universitat de Girona
Campus Montilivi, 17071 Girona (Spain)
E-mail: albert.poater@udg.edu

[c] Prof. L. Cavallo
KAUST Catalysis Center
4700 King Abdullah University of Science and Technology
Thuwal 23955-6900 (Kingdom of Saudi Arabia)

Supporting information for this article is available on the WWW under http://dx.doi.org/10.1002/chem.201304699.

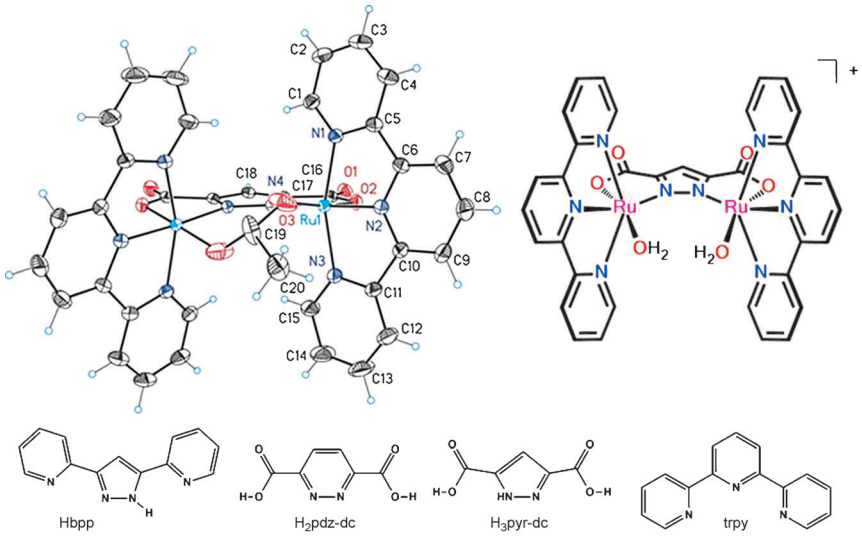

Figure 1. Top left: Ortep plot of the X-ray crystal structure of **1** (ellipsoid at 50% probability). Top right: drawn structure of complex $\mathbf{2}^{+}$. Bottom: drawn structures of the discussed ligands.

A quantitative evaluation of this effect can be obtained upon comparison of their redox potentials with those of analogous complexes containing the monoanionic bpp^{-} ligand (3,5-bis(2-pyridyl)pyrazole anion) $\{[Ru^{II}(trpy)(H_2O)]_2(\mu\text{-}bpp)\}^{3+}$, $\mathbf{4}^{3+}$, and the dianionic pdz-dc^{2-} (pyridazine-3,6-dicarboxylato) $\{[Ru^{II}(trpy)(H_2O)]_2(\mu\text{-}pdz\text{-}dc)\}^{2+}$, $\mathbf{5}^{2+}$.[24] For $\mathbf{2}^{+}$, this strong electron donating effect renders a cathodic shift of 390, 300, 120, and 130 mV to the III–II,II–II, III–III,III–II, IV–III,III,III, and IV–IV,IV–III redox potentials respectively with regard to $\mathbf{4}^{3+}$ (see Table S1 in the Supporting Information). The capacity of complex $\mathbf{2}^{+}$ to epoxidize alkenes is spectacular. Table 2 shows the results of epoxidation reactions for a variety of alkenes using PhIO as oxidant in a mixture of CH_2Cl_2/EtOH/H_2O as solvent with cat./subs ratios of 1:2000. As an example, *cis*-cyclooctene and cyclohexene (Table 1, entries 1 and 2) are nearly quantitatively oxidized to their corresponding oxides with impressive TOFs of 22320 and 24240 cycles per hour which are the best ever reported for Ru complexes and within the best reported for other transition metal complexes.[18–23] Other alkenes containing aliphatic and/or aromatic substituents are also very efficiently oxidized as displayed in Table 2. In general, the more electron rich alkene the faster the reaction indicating an electrophilic character of the Ru–O active site, as is also the case for related Ru epoxidation catalysts.[24–26]

It is interesting to point out here that $\mathbf{2}^{+}$, under comparable conditions, is about two orders of magnitude faster than its mononuclear analogue trans-$[Ru^{II}(pic)(trpy)(H_2O)]^{+}$, $\mathbf{6}^{+}$ (pic = picolinato ligand)[27] and 20 times faster than the related dinuclear complex $\mathbf{5}^{2+}$ containing the dianionic ligand pdz-dc^{2-}.[24b] These comparative results manifest the synergistic effects of the accessibility of higher oxidation states, thanks to the σ-donating nature of the ligands, combined with the cooperative effect of a properly designed complex with two metal sites strategically situated.

A very interesting feature of this catalyst is its capacity to oxidize *cis*-alkenes stereospecifically to their corresponding *cis*-epoxides without any isomerization. Yet the most striking feature of our system is the different reactivity displayed by $\mathbf{2}^{+}$ with regard to *cis*- and *trans*-alkene isomers. While the relative rate of oxidation of *cis*- and *trans*-β-methylstyrene are relatively similar, for 2-octene the *cis* is oxidized about roughly 5 times faster than the *trans* and for stilbene it is just the other way around, that is, the *trans* isomer is oxidized about 3 times faster than the *cis* isomer. Given the nearly identical electronic nature of the *cis* and *trans* alkenes, the differential reactivity can only be due to a supramolecular effect. To understand and rationalize the origin of this differentiated reactivity we carried out a DFT characterization of the whole catalytic system (see below). To gather insight into the

Table 1. Catalytic performance of $\mathbf{2}^{+}$ for the epoxidation of several alkenes using PhIO.[a]

Entry	Alkene	Conv. [%]	Epoxide [M] Selectivity [%][b]	TN/TOF_i[c]
1	*cis*-cyclooctene	100	1.88 (94)	1880/22320
2	cyclohexene	100	1.94 (97)	1940/24240
3	styrene	99	1.15 (58)	1150/10380
4	α-Me-styrene	100	0.98 (49)	980/9180
5	*cis*-β-Me-styrene	100	1.74 (87)[d]	1740/14400
6	*trans*-β-Me-styrene	100	1.8 (90)[e]	1800/18540
7	*cis*-2-octene	100	1.92 (96)[d]	1920/21900
8	*trans*-2-octene	87	1.15 (66)[e]	1150/4500
9	*cis*-stilbene[f]	32	0.26 (40)[d]	130/3852
10	*trans*-stilbene[f]	61	0.70 (57)[e]	350/10260
11	triphenylethylene	25	0.24 (48)	240/2640

[a] Reaction conditions: $\mathbf{2}^{+}$ (1.0 mM), alkene (2.0 M), $PhI(OAc)_2$ (4.0 M), H_2O (4.0 M), dodecane (165 mM), DCM/EtOH (1:1) up to a final volume of 1.3 mL. [b] Epoxide selectivity = [epoxide]final/{[substrate]initial − [substrate]final}·100. [c] TN is the turnover number with regard to the epoxide. TOF_i is the initial turnover frequency expressed in epoxide cycles per hour. [d] 100% of *cis*-epoxide. [e] 100% of *trans*-epoxide. [f] Ratio cat./subs/ox/water = 1:1000:2000:2000.

Table 2. Relative energies with respect to initial substrate and catalyst A, in kcal mol^{-1}, of the most stable epoxidation pathway.

	$\mathbf{A}^{Q}$	$\mathbf{TS(A \rightarrow B)}^{Q[a]}$	$\Delta_{cis-trans}$
cis-stilbene	0.0	21.0	
trans-stilbene	0.0	20.3	0.7
cis-β-Me-styrene	0.0	18.4	
trans-β-Me-styrene	0.0	18.1	0.3
cis-2-octene	0.0	22.8	
trans-2-octene	0.0	24.9	−2.1

[a] Q = quintuplet, refers to the multiplicity of the ground state.

nature of the reactive species involved in the catalytic cycle we carried out electrochemical experiments with the catalyst in the presence and absence of styrene (see Figure S4 in the Supporting Information). These experiments clearly show that while lower oxidation states are not sensitive to the presence of styrene, when the catalyst reaches oxidation state IV–IV, a large electrocatalytic wave is observed due to the oxidation of styrene to styrene oxide. Since this oxidation is basically a two-electron process, and given the significant electronic coupling between the two metal centers, the reaction that takes place can be written as follows (the trpy and pyr-dc^{3-} ligands have been omitted for clarity):

$$[(O)Ru^{IV}Ru^{IV}(O)]^{+}+PhCH{=}CH_2+H_2O \rightarrow [(OH)Ru^{III}Ru^{III}OH]^{+}+PhCH(O)CH_2$$

With this information in hand we carried out DFT calculations to characterize the complete catalytic cycle for the oxidized $\mathbf{2}^{+}$ at oxidation state IV,IV;[28] that is, the $[(O)Ru^{IV}Ru^{IV}(O)]^{+}$ species. A graphic summary of the mechanism is represented in the upper part of Figure 2 for the oxidation of *cis*-β-methylstyrene, starting from the $[(O)Ru^{IV}Ru^{IV}(O)]^{+}$ species, **A**.

The first step that turns out to be the rate determining step involves the interaction of the double bond of the alkene with one of the Ru=O groups that eventually will transfer the O-atom to the alkene. In addition, in transition state **TS(A→B)** the catalyst also interacts with the substrate through the second Ru=O group producing a supramolecular H-bond interaction with the aliphatic and/or aromatic substituents of the alkene. The latter is the key differentiating phenomena that dictates the relative rates of oxidation of the *cis*/*trans* isomers and thus the stereoselective preferences of the catalyst. This second Ru=O group is situated in a cavity shielded by the trpy ligands and thus the degree of interaction with a particular substrate will depend on the accommodation capacity of the substrate (steric effects) within the cavity together with the substrate capacity to generate H-interactions with this second Ru=O group. Once species **B** is formed with the oxygen atom of the first Ru–O group bonded to one of the carbon atoms of the alkene, then it reorients through a very low energy step (**TS(B→C)**) to finally collapse to the second C-atom of the alkene generating the epoxide **C**. The complete DFT catalytic cycle for *cis*–*trans* 2-octene, *cis*–*trans* β-methylstyrene and *cis*–*trans* stilbene has been calculated to evaluate the steric and electronic parameters involved, which can lead to an understanding of their differentiated stereoselectivity, and the data is displayed in Table 2.

The results agree well with the experimental *cis*–*trans* stereoselectivities obtained experimentally in the sense that follow the same trends. Figure 2 bottom shows the structures of the **TS(A→B)** obtained for the case of *cis*- and *trans*-2-octene isomers, that differ by 2.1 kcal mol^{-1}. From their relative metric parameters it can be observed that the *cis* isomer generates two significant H-interactions (O2-H5b, 2.324 Å; O2-H3, 2.655 Å) compared to just one for the *trans* isomer (O2-H2, 2.401 Å). The sterics involved in the cavity together with the stronger interaction of the *cis* are thus responsible for lowering the **TS(A→B)** energy and as a consequence the oxidation of the *cis*-isomer occurs at a faster rate than the *trans*. To better show the cavity generated by the catalyst $\mathbf{2}^{+}$, a topographic steric map has been generated (Figure 3), in which the pyridyl groups of each trpy ligand are labeled (trpy1 with py1, py2,

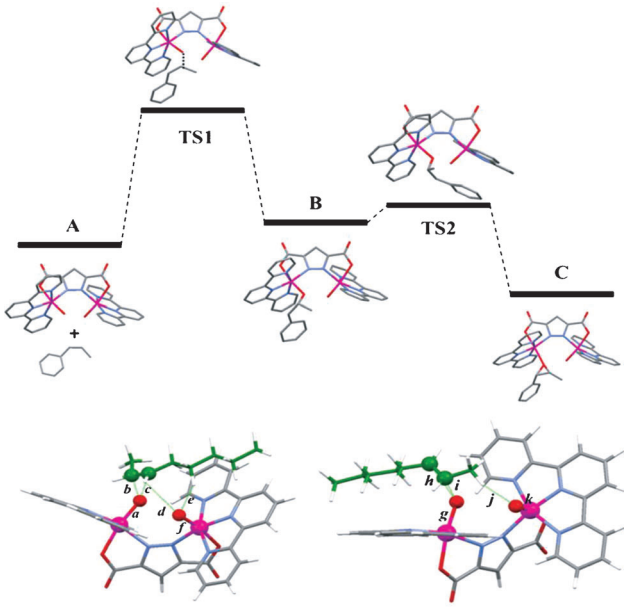

Figure 2. Top: DFT stationary points located along the reaction path for the reaction of oxidized $\mathbf{2}^{+}$ with *cis*-β-methylstyrene (energies in kcal mol^{-1}, H atoms omitted for clarity). Bottom: mixed ball and stick representation of the DFT calculated **TS(A→B)** for *cis*-2-octene (left) and *trans*-2-octene (right). Color code: Ru magenta, N blue, O red, C gray, and H white. For clarity, the carbon backbone of the substrate is labeled in green and the C=C and Ru=O moieties are shown as balls. Interesting metric parameters in Å: a = 1.853, b = 1.967, c = 2.610, d = 2.655, e = 2.324, f = 1.799, g = 1.860, h = 1.902, i = 1.863, j = 2.401, k = 1.796.

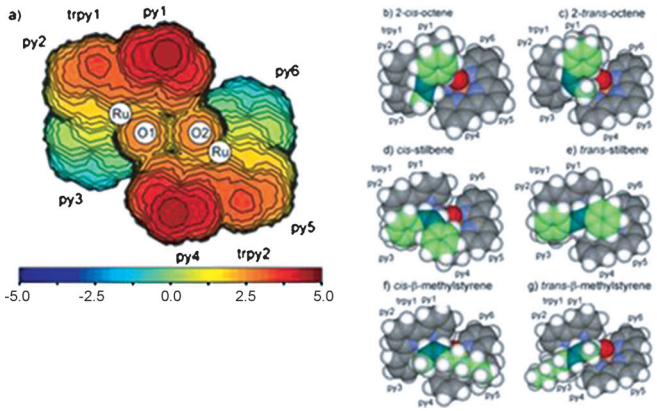

Figure 3. a) Topographic steric map of the $[(O)Ru^{IV}Ru^{IV}(O)]^{+}$ species of the catalyst. The isocontour levels scale (Å) is also indicated. The py (n = 1–6), labels refer to the different pyridyl groups of the trpy1 and trpy2 ligands. b–g) Van der Waals representation of the transition states for the attack of 2-octene at the O atom of the Ru–O1 moiety. For clarity, the C atoms of the C=C bond of the substrate are colored in dark green, while the other C atoms of the substrate are in pale green. The O and Ru atoms are colored in red and orange, respectively.

and py3 and trpy2 with py4, py5, and py6).[29] The map clearly indicates the almost C2 symmetric folding of the two trpy ligands, to form a narrow groove hosting the two O atoms of the Ru–O moieties. The py1 and py4 pyridyl rings of trpy1 and trpy2 flank the Ru–O1 and Ru–O2 groups, limiting substrate accessibility to the Ru–O functionality. Py2 and py5 offer some additional shielding to Ru–O1 and Ru–O2 respectively, whereas py3 and py6 are oriented downwards. Selectivity in favor of the *cis* or *trans* isomer of the substrate is of course determined by the ability of the alkene isomers to adapt better to the reactive pocket of the catalyst. A van der Waals representation of the six key transition states is reported in Figure 3 (right panel). In all cases, the substrate is attacking the O atom of the Ru–O1 metal bonded to the trpy1 moiety whereas the Ru–O2 moiety bonded to tpry2 is responsible for hydrogen interaction with the substrate only. For *cis*-2-octene, both the Me and the *n*-pentyl groups of the alkene are pointing away from the trpy1 ligand, with the *n*-pentyl protruding above py5 of trpy2. Differently, for *trans*-2-octene the transition state presents the *n*-pentyl tail protruding away from the catalyst right above py3. The main difference between the two transition states is in the orientation of the C=C double bond of the substrate. As a consequence of this, the alkene C-atom forming the C–O bond is oriented away from the discriminating Ru–O2 unit in the *trans* transition state, while it is oriented inwards in the favored *cis* transition state. In the latter case, the distance between the C–O forming C atom and the O2 atom is only 3.11 Å. Considering the high electrophilicity of the Ru–O bond, the higher stability of the *cis*-transition state is also improved by a favorable interaction between this C–O forming C atom and the Ru–O1 bond, which works in a synergic manner with the previously mentioned H-bond between the substrate and the Ru–O moiety.

For stilbene, the Ph ring bound to the C atom of the forming C–O bond is involved in a π-stacking interaction with the aromatic plane of the trpy1 ligand in both the *cis* and the *trans* transition states, with a rather similar orientation. This suggests that the selectivity between *cis* and *trans* isomers is related to the significantly different interaction of the second Ph group attached to the other C atom (see Figure 3). The main difference is in the Ph ring attached to the C-atom of the non-forming C–O bond. In the *cis* transition state, this ring has a π-stacking interaction with py4, while in the favored *trans* transition state it has an interaction through the O2 atom (3.03 Å distance between the C-ipso atoms of the Ph ring and the O2 atom). It is worth mentioning here that in both transition states, the C atom forming the initial C–O bond is located quite away from the O2 atom, 3.30 and 3.56 Å in *cis* and *trans* transition states, respectively. Overall a common feature for the favored transition states for 2-octene and stilbene is the interaction of the substrate with the O-atom of the Ru-O2 bond, thus pointing out that the selectivity is basically dictated by this supramolecular interaction.

Finally, for *cis*- and *trans*-β-Me-styrene, the Ph ring is involved in a π-stacking interaction with the trpy1 unit in both transition states, and the relative orientation of the two moieties is relatively similar in both transition states. The only difference between these two transition states is in the relative disposition of the H and Me groups at the C-β atom. In the *cis* transition state is oriented towards the py4 unit, whereas in the *trans* transition state it is oriented towards the py3 unit. However, in both transition states the Me group is located quite away from them, with minimum distance around 3.4 Å, so that the Me group is unable to generate any selectivity. As a consequence of all this the *cis* and *trans* isomers have comparable epoxidation rates.

In conclusion, we have prepared a new dinuclear $Ru–OH_2$ complex, $\mathbf{2}^{+}$, that thanks to the trianionic ligand backbone ($pyr\text{-}dc^{3-}$) can easily reach the IV,IV high oxidation state, which is extremely powerful for the epoxidation of a variety of alkenes. The oxidized dinuclear complex $\mathbf{2}^{+}$ in oxidation state IV,IV, behaves in a stereoselective manner thanks to the different role of the two Ru=O groups. While one of them is responsible for oxygen transfer, the second one is partly responsible for a supramolecular interaction. The latter is also influenced by the ligand architecture that generates a discriminating pocket for the incoming substrate. The combination of these factors enables oxidized $\mathbf{2}^{+}$ to behave as a stereoselective supramolecular oxidation catalyst without the need to use specific modifications of the substrates. The present work constitutes the first example of this new paradigm in supramolecular oxidation catalysis and could be extendable to a large variety of instances.

Acknowledgements

This research was supported financially by MINECO (CTQ2011-23156/BQU, CTQ2010-21497 and PRI-PIBIN-2011-1278), ICIQ, FEDER fund (UNGI08-4E-003), ICREA Academia, Generalitat de Catalunya (2009SGR637); Ramón y Cajal contract (RYC-2009-05226) of MINECO, and Career Integration Grant (CIG09-GA-2011-293900) of the European Commission. COST Actions CM1205 and CM1202 are also gratefully acknowledged.

Keywords: density functional calculations · electrochemistry · epoxidation · ruthenium · supramolecular redox catalysis

[1] M. L. Clarke, J. A. Fuentes, *Angew. Chem.* **2007**, *122*, 9383; *Angew. Chem. Int. Ed.* **2007**, *46*, 930.
[2] T. Šmejkal, B. Breit, *Angew. Chem.* **2008**, *120*, 4010; *Angew. Chem. Int. Ed.* **2008**, *47*, 3946.
[3] J. Meeuwissen, J. N. H. Reek, *Nat. Chem.* **2010**, *2*, 615.
[4] Y. Wang, T.-Y. Yu, H.-B. Zhang, Y.-C. Luo, P.-F. Xu, *Angew. Chem. Int. Ed.* **2012**, *51*, 12339.
[5] J. Park, K. Lang, K. A. Abboud, S. J. Hong, *J. Am. Chem. Soc.* **2008**, *130*, 16484.
[6] S. Das, C. D. Incarvito, R. H. Crabtree, G. W. Brudvig, *Science* **2006**, *312*, 1941.
[7] Z. Fang, R. Breslow, *Org. Lett.* **2006**, *8*, 251.
[8] J. Yang, R. Breslow, *Angew. Chem.* **2000**, *112*, 2804; *Angew. Chem. Int. Ed.* **2000**, *39*, 2692.
[9] R. Breslow, X. Zhang, Y. Huang, *J. Am. Chem. Soc.* **1997**, *119*, 4535.
[10] P. Fackler, C. Berthold, F. Voss, T. Bach, *J. Am. Chem. Soc.* **2010**, *132*, 15911.
[11] S. J. Lee, S.-H. Cho, K. L. Mulfort, D. M. Tiede, J. T. Hupp, S. T. Nguyen, *J. Am. Chem. Soc.* **2008**, *130*, 16828.

[12] O. Perraud, A. B. Sorokin, J.-P. Dutasta, A. Martinez, *Chem. Commun.* **2013**, *49*, 1288.
[13] a) W. I. Dzik, X. Xu, X. P. Zhang, J. N. H. Reek, B. de Bruin, *J. Am. Chem. Soc.* **2010**, *132*, 10891; b) P. Dydio, J. H. N. Reek, *Angew. Chem. Int. Ed.* **2013**, *52*, 3878; c) T. Šmejkal, B. Breit, *Angew. Chem.* **2008**, *120*, 317; *Angew. Chem. Int. Ed.* **2008**, *47*, 311; d) P. Dydio, W. I. Dzik, M. Lutz, B. de Bruin, J. H. N. Reek, *Angew. Chem.* **2011**, *123*, 416; *Angew. Chem. Int. Ed.* **2011**, *50*, 396; e) L. Du, P. Cao, J. Xing, Y. Lou, L. Jiang, L. Li, J. Liao, *Angew. Chem. Int. Ed.* **2013**, *52*, 4207; f) L. Pignataro, S. Carboni, M. Civera, R. Colombo, U. Piarulli, C. Gennari, *Angew. Chem.* **2010**, *122*, 6783; *Angew. Chem. Int. Ed.* **2010**, *49*, 6633; g) P.-A. R. Breuil, F. W. Patureau, J. N. H. Reek, *Angew. Chem.* **2009**, *121*, 2196; *Angew. Chem. Int. Ed.* **2009**, *48*, 2162; h) C. Anda, A. Llobet, V. Salvado, R. Motekaitis, J. Riebenspies, A. E. Martell, *Inorg. Chem.* **2000**, *39*, 2986 – 2999.
[14] W. R. Browne, R. Hage, J. G. Vos, *Coord. Chem. Rev.* **2006**, *250*, 1653.
[15] S. Roeser, M. Z. Ertem, C. Cady, R. Lomoth, J. Benet-Buchholz, L. Hammarstrom, B. Sarkar, W. Kaim, C. J. Cramer, A. Llobet, *Inorg. Chem.* **2012**, *51*, 320.
[16] N. Planas, G. Christian, S. Roeser, E. Mas-Marza, M.-R. Kollipara, J. Benet-Buchholz, F. Maseras, A. Llobet, *Inorg. Chem.* **2012**, *51*, 1889.
[17] J. Mola, C. Dinoi, X. Sala, M. Rodriguez, I. Romero, T. Parella, X. Fontrodona, A. Llobet, *Dalton Trans.* **2011**, *40*, 3640.
[18] S. Yu, C.-X. Miao, D. Wang, S. Wang, C. Xia, W. Sun, *J. Mol. Catal. A* **2012**, *353 – 354*, 185.
[19] F. Romano, A. Linden, M. Mba, C. Zonta, G. Licini, *Adv. Synth. Catal.* **2010**, *352*, 2937.
[20] P. Liu, H. Wang, P. Ying, C. Li, *J. Catal.* **2008**, *256*, 345.
[21] S. Krackl, A. Company, S. Enthaler, M. Driess, *ChemCatChem* **2011**, *3*, 1186.
[22] S. A. Hauser, M. Cokoja, F. E. Kuhn, *Catal. Sci. Technol.* **2013**, *3*, 552.
[23] H. Agarwala, F. Ehret, A. D. Chowdhury, S. Maji, S. M. Mobin, W. Kaim, G. K. Lahiri, *Dalton Trans.* **2013**, *42*, 3721.
[24] a) C. Sens, I. Romero, M. Rodríguez, A. Llobet, T. Parella, J. Benet-Buchholz, *J. Am. Chem. Soc.* **2004**, *126*, 7798; b) C. Di Giovanni, L. Vaquer, X. Sala, J. Benet-Buchholz, A. Llobet, *Inorg. Chem.* **2013**, *52*, 4335.
[25] I. Serrano, M. I. López, I. Ferrer, A. Poater, T. Parella, X. Fontrodona, M. Solà, A. Llobet, M. Rodríguez, I. Romero, *Inorg. Chem.* **2011**, *50*, 6044.
[26] W. Mägerlein, C. Dreisbach, H. Hugl, M. K. Tse, M. Klawonn, S. Bhor, M. Beller, *Catal. Today* **2007**, *121*, 140.
[27] A. Llobet, P. Doppelt, T. J. Meyer, *Inorg. Chem.* **1988**, *27*, 514.
[28] For DFT details see the supporting information.
[29] F. Ragone, A. Poater, L. Cavallo, *J. Am. Chem. Soc.* **2010**, *132*, 4249.

Received: November 30, 2013
Published online on March 3, 2014